Platinum nanoparticles stabilized by CO and octanethiol ligands or polymers: FT-IR, NMR, HREM and WAXS studies

Fabrice Dassenoy,[a] Karine Philippot,[b] Teyeb Ould Ely,[b] Catherine Amiens,[b] Pierre Lecante,[a] Etienne Snoeck,[a] Alain Mosset,[a] Marie-José Casanove,*,[†],[a] and Bruno Chaudret*,[‡],[b]

[a] Centre d'Elaboration des Matériaux et d'Etudes Structurales du CNRS, 29, rue Jeanne Marvig, BP 4347, 31055 Toulouse cédex, France
[b] Laboratoire de Chimie de Coordination du CNRS, 205, route de Narbonne, 31077 Toulouse cédex, France

The reaction of $Pt_2(dba)_3$ with CO leads rapidly to the formation of platinum nanoparticles. Stabilization of the particles was achieved by octanethiol or various polymers. Spectroscopic studies demonstrate the coordination of thiol at the surface of the particles. The size distribution is *quasi* monodisperse and centered near 1.6 ± 0.15 nm as demonstrated by HREM. However, only the core of the particles is crystalline, the outer shell being heavily disordered as demonstrated both by HREM and WAXS. This disorder is attributed to the influence of strongly coordinating ligands. For comparison, HREM and WAXS data were recorded on platinum nanoparticles prepared in various polymers: polyvinylpyrrolidone (PVP), nitrocellulose (NC) and cellulose acetate (CA). In addition, a sample has been obtained from decomposition of $Pt_2(dba)_3$ by dihydrogen in PVP. The particles are well-crystallized and display HREM sizes that vary as a function of the polymer: <1 nm (PVP/CO), 1.30 ± 0.15 nm (NC), 1.70 ± 0.15 nm (CA) and 1.50 ± 0.15 nm (PVP/H$_2$). Models elaborated from WAXS data recorded on these different colloids are in agreement with the presence of, respectively, one-shell clusters, a mixture of two- and three-shell clusters (85 : 15), a mixture of three- and four-shell clusters (80 : 20) and three-shell clusters. There is little or no discrepancy between the HREM and WAXS data in these cases, hence demonstrating the absence of strong interactions between the polymers and the surface. The best fit was obtained for the colloid prepared under H$_2$ in PVP, which resembles a free platinum nanoparticle, whereas the colloid stabilized by thiol(ate) ligands behaves as a 'giant cluster'.

Nanoparticules de platine stabilisées par le monoxyde de carbone et des ligands octanethiol ou des polymères: études IR-FT, RMN, MEHR et WAXS. La réaction du complexe $Pt_2(dba)_3$ avec CO conduit rapidement à des nanoparticules de platine qui ont été stabilisées par l'utilisation d'octanethiol ou de polymères variés. Les études spectroscopiques démontrent la coordination du thiol à la surface des particules. En microscopie électronique à haute résolution (MEHR), la distribution de tailles est *quasi* monodisperse et centrée à $1{,}60 \pm 0{,}15$ nm. Les études MEHR et WAXS montrent que seul le coeur est bien cristallisé, la couche externe étant très désordonnée. Ce désordre est attribué à l'influence des ligands thiol fortement coordinants. Pour comparaison, des études MEHR et WAXS ont été réalisées sur des particules de platine préparées dans différents polymères: polyvinylpyrrolidone (PVP), nitrocellulose (NC) et acétate de cellulose (AC). Un autre composé a également été synthétisé par décomposition du précurseur $Pt_2(dba)_3$ sous H$_2$ en présence de PVP. Les particules obtenues sont bien cristallisées et présentent des tailles MEHR qui varient en fonction du polymère [<1 nm (PVP/CO), $1{,}30 \pm 0{,}15$ nm (NC/CO), $1{,}70 \pm 0{,}15$ nm (AC/CO) et $1{,}50 \pm 0{,}15$ nm (PVP/H$_2$)] et qui correspondent respectivement à des modèles en WAXS contenant des clusters à une couche, un mélange de clusters à 2 et 3 couches (85 : 15), un mélange de clusters à 3 et 4 couches (80 : 20) et des clusters à 3 couches. Dans ces cas, il y a peu ou pas de contradiction entre les données MEHR et WAXS, ce qui démontre l'absence d'interaction forte entre les polymères et la surface. Le meilleur accord a été obtenu pour le colloïde préparé sous H$_2$ dans la PVP. Ce colloïde ressemble à une nanoparticule libre alors que le colloïde stabilisé par les ligands thiol(ate)s se comporte comme une cluster géante.

The physical and chemical properties of transition metal nanoparticles or of oxides or sulfides with sizes at the frontier between the molecular and the solid state are of great fundamental interest.[1] These materials can also be of practical use in the fields of catalysis[2,3] or materials science [4] as semiconductors, superparamagnets, gas sensors, etc. However, in order to understand and adjust the properties of such materials in the field of catalysis, the particles must have a controlled size, a controlled surface composition and be stable under the reaction conditions. The first two conditions must also be fulfilled for their use in materials science but in addition, the bulk structure of the material made from the nanoparticles must also be controlled, either by self-assembly processes[5–7] or by manipulation of the nanoclusters as 'superatoms'.

During the past few years we have addressed the problem of the synthesis of nanoparticles of controlled size and surface composition through an organometallic approach.[8–12] It has, for example, been possible to synthesize platinum particles displaying a very narrow size distribution centered around 1.2 nm.[10] We have demonstrated on this occasion that the par-

† Fax: +33 562257999. E-mail: casanove@cemes.fr
‡ Fax: +33 561553003. E-mail: chaudret@lcc-toulouse.fr

ticles adopt, in general, the bulk fcc structure, except if sterically demanding phosphine ligands force the particle to adopt an icosahedral structure.[10] However, we have also shown that using CO, THF, PPh₃ or THT ligands we could not sufficiently stabilize the particles in solution for further use.[10,11]

In order to obtain stable particles, we considered using thiolate ligands. Thiolates have been commonly used to stabilize gold colloids[5,13,14] prepared in general by the reduction of metal salts. The colloidal solutions obtained with this procedure have proven to be stable and furthermore to self-assemble on surfaces or even in solution. Bisthiolate ligands have even been used to link together individual clusters.[7] Few examples of the stabilization of platinum particles by thiolate ligands[15] are known and these concern particles of large size.

During the course of the present study, we observed a discrepancy between the results of the particle characterization by WAXS and HREM techniques. This discrepancy could be the result of a strong interaction between surface ligands and surface atoms leading to a distorsion of the structure of the particle. In order to study this phenomenon we reinvestigated the size and structure of platinum particles dispersed in various polymers [polyvinylpyrrolidone (PVP), nitrocellulose (NC), cellulose acetate (CA)].

We describe in this paper the synthesis of new platinum nanoparticles stabilized by octanethiol ligands and their characterization by WAXS (wide angle X-ray scattering) and HREM (high resolution electron microscopy), as well as a comparison of these results with those obtained for platinum particles sterically protected in polymers.

Results

Synthesis and characterization of octanethiol-stabilized platinum nanoparticles

Previous studies[8-11] in the group have demonstrated that addition of CO on a solution of the precursor $Pt_2(dba)_3$[16] led rapidly to the formation of platinum nanoparticles. However, the nature of the colloidal solution prepared in this way is highly dependent upon the solvent[10] in which the reaction is carried out. In toluene, a brown powder precipitated and it was shown to contain fcc platinum particles displaying a broad size distribution (**Colloid 1**). In contrast to this result, in THF a homogeneous solution shown to contain nearly monodisperse platinum particles with a mean size of *ca.* 1.2 nm (**Colloid 2**) was obtained. Conversion of **Colloid 1** into **Colloid 2** was rapid in THF. For the purpose of the present work, we added thiols on both species.

Addition of 0.2 equiv. octanethiol per Pt to the precipitate of platinum particles obtained in toluene (**Colloid 1**) leads to a brown suspension. The mixture was subjected to ultrasound in a bath for 1 hour and left stirring in solution for 3 days to achieve dissolution, thus leading to a colloid hereafter named **Colloid 3**. Infrared monitoring of the reaction mixture indicated the presence of two absorption bands at 2051 and 1810 cm⁻¹ after sonication. These bands are those of **Colloid 1**, which indicates that coordination of thiol has not yet occurred. The terminal CO stretch shifts to 2047 cm⁻¹ after 2 days, and to 2039 cm⁻¹ after 3 days, in agreement with coverage of the surface by the thiol ligands, whereas the bridging CO becomes hardly visible (Fig. 1). It was not possible to observe the S—H stretching bands due to their low intensity. HREM analysis of the colloidal solution shows the presence of particles displaying a relatively broad size distribution and a mean size of 1.4 nm (Fig. 2).

Adding 0.2 equiv. octanethiol on a platinum colloid prepared in THF (**Colloid 2**) produces rapidly a homogeneous brown solution exhibiting two infrared bands at 2040 and 1799 cm⁻¹ (Fig. 3), close to the values found for the **Colloid 3**. It is noteworthy that thiol addition leads to a decrease
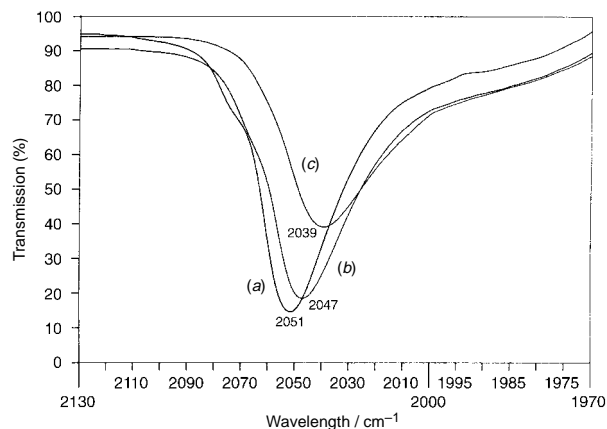
Fig. 1 Infrared monitoring of the reaction mixture obtained after addition of octanethiol to **Colloid 1**: (curve *a*) after 2 h, (curve *b*) after 2 days, showing the evolution to **Colloid 3** (curve *c*) after 3 days

in the intensity of the CO stretching band and to a low frequency shift, in agreement with CO substitution and the presence of a more electron-rich platinum surface. Evaporation to dryness of the solution leads to the formation of a brown powder, very soluble in common organic solvents such as THF and pentane, hereafter named **Colloid 4**. A microanalysis carried out on this powder demonstrates the presence of a large amount of solvent and of dba residues in the colloid. However, it was possible to determine a platinum : sulfur ratio of 4.34 : 1. The same reaction carried out on a sample of colloid prepared and purified in toluene and then redissolved in THF before the addition of 0.2 equiv. octanethiol per Pt essentially
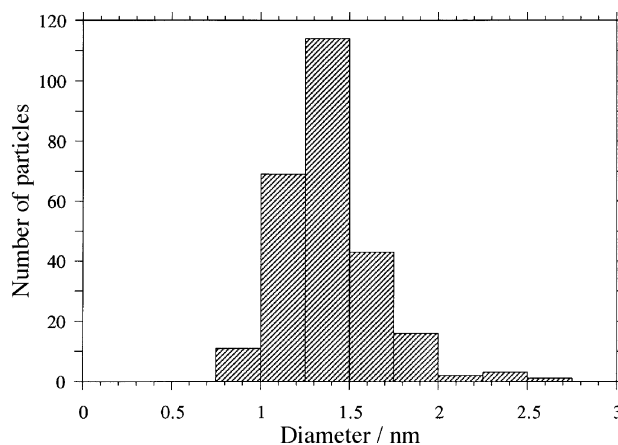
Fig. 2 Histogram of the sizes of **Colloid 3** determined from HREM showing a broad size distribution and a mean size of 1.4 nm
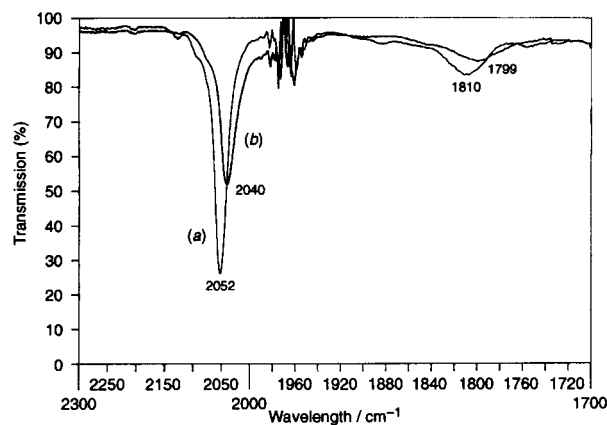
Fig. 3 Infrared spectra of **Colloids 2** (curve *a*) and **4** (curve *b*)

led to the same result. Analysis by high resolution electron microscopy of **Colloid 4** solutions resulting from three different preparations demonstrated the presence of disordered platinum nanoparticles of a mean size centered near 1.6 nm. The micrograph in Fig. 4(a) shows that the particles all have roughly the same size and that there is no overlap or
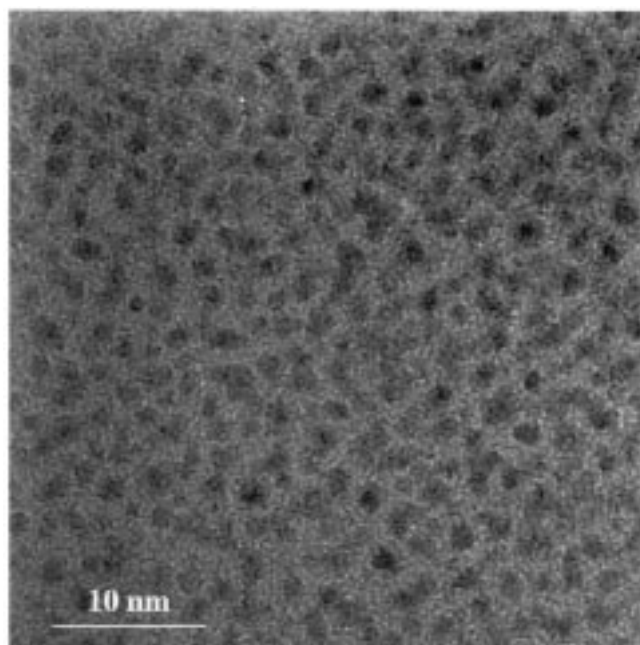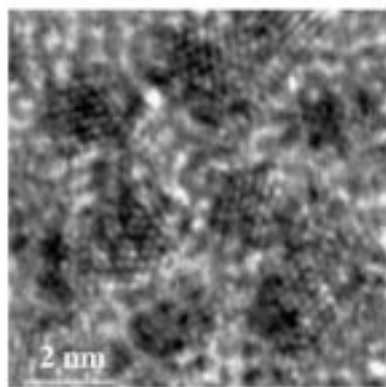
coalescence of individual particles. The histogram (Fig. 5) shows that the size distribution of **Colloid 4** is extremely narrow and, given the measurement errors,[17] can be considered as monodisperse. The origin of this monodispersity for a size suggesting the presence of mostly three-shell clusters is not clear but could result from a size adjustment, allowing the most satisfactory coverage of the surface by the thiol groups. Furthermore, Fig. 4(b) shows that nearby particles do not coalesce but remain separated quite regularly by a distance of *ca.* 0.7 nm. This arrangement of the particles is most probably due to the presence of the protecting octanethiol ligands and the separation distance indicates that their coordination spheres are imbricated into one another through self-assembly. **Colloid 4** is very stable; it can be kept in solution for several weeks without decomposition; it can also be isolated and redissolved without any change in its properties. This stability is clearly a result of the presence of the thiol groups, however, we do not know whether the sulfur ligands are coordinated as thiol or thiolate groups. Given the much higher stability of **Colloid 4** compared to the corresponding colloid stabilized by THT, we favour the presence of thiolate groups at the surface.

^{1}H and ^{13}C NMR spectra of this colloid were measured in [^{2}H$_8$]THF (400 MHz, 293 K). The ^{13}C{^{1}H} NMR spectrum shows broad peaks at 14.9, 24.0, 30.6 and 33.3 ppm, which can be attributed by comparison to the spectrum of free octanethiol to the methyl group (C8) of the thiol chain, to the methylene C7, to two overlapping methylene groups, namely C4 and C5, and to the methylene group C6, respectively. The α, β and γ carbons (C1, C2 and C3) are not seen, probably as a result of shielding by the platinum particle. A similar effect has been recently observed by Reven and colleagues in alkanethiol-capped gold colloids.[14] Interestingly, these authors were also unable to locate the resonances of the three α, β and γ carbons. At each position, it is possible to observe both a broad resonance assigned to the coordinated octanethiol and a minor sharp one assigned to the free ligand. These resonances do not exchange, which suggests that there is no exchange between free and coordinated octanethiol and moreover, the amount of free ligand is very small compared to the complexed one. The ^{1}H NMR spectrum is less informative but peaks at 0.85 and *ca.* 1.3 ppm corresponding to the methyl group (C8) and some methylene groups of the octanethiol ligand could be observed. It was not possible, using spectroscopic techniques, to determine whether the thiol molecules are coordinated unchanged or are transformed into thiolate groups.

In order to characterize the particles present in **Colloid 4** fully, we carried out an analysis of the product by WAXS. This technique allows one to determine the particle crystal structure and a coherence length corresponding to the ordering within a given particle, hence leading to a model of cluster size. For convenience, the models we use are closed-shell clusters having a 'magic' number of atoms or a combination of two such clusters. In reality, it is doubtless that there is a distribution in atom numbers. Measurements carried out both on the brown precipitate and on a THF solution (after correction for solvent contributions) leads to a well-defined reduced radial distribution function (RDF) consistent with a small cuboctahedral model (Fig. 6). The structure is fcc and the apparent size of the particles is consistent with a model including a mixture of 13- and 55-atom cuboctahedral particles in a 95 : 5 ratio. The Pt—Pt distance (0.2775 nm) is similar to that found for bulk platinum and a value of 7×10^{-5} nm^{-2} has been affected to the individual b_i dispersion factors. However, a mixture of particles containing three- and four-shell clusters was expected from HREM. The same problem was encountered with THT-protected platinum nanoparticles of 1.3 nm mean size but for which the best fit of the WAXS data was obtained with a 13-atom model.[11] This

Fig. 4 (a) HREM micrograph of **Colloid 4** showing that the particles have all roughly the same size and that they are regularly separated; (b) nearby particles with no coalescence
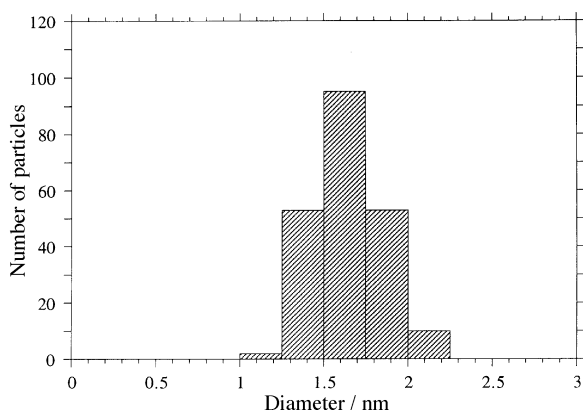

Fig. 5 Histogram of the sizes of **Colloid 4** determined from HREM showing a narrow size distribution and a mean size of 1.6 nm
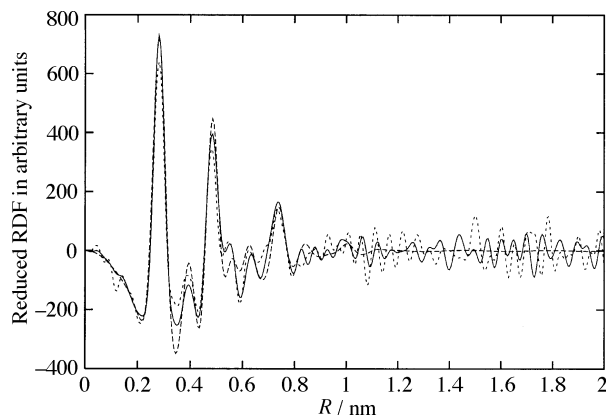
Fig. 6 RDF of particles of **Colloid 4** (solid line: experimental data obtained in solution in THF; thick broken line: cuboctahedral model; thin broken line: experimental data obtained from powder)

problem was not encountered for **Colloid 2** for which the RDF was consistent with a fcc model containing mostly 55 atoms, in agreement with the HREM analysis showing the presence of very small crystalline fcc particles of mean size 1.2 nm.[10]

The difference between the THT- or octanethiol-protected platinum particles and the THF-protected ones is the presence, at the surface, of a very good donor ligand that can modify the arrangement of the surface atoms. The WAXS analysis would then emphasize the crystalline environment located in the center of the particles.

Characterization by WAXS and HREM of platinum nanoparticles stabilized by various polymers

The discrepancy described in the preceding chapter between HREM and WAXS results led us to reconsider previous work[9] on the stabilization of particles in polymers. It is expected that polymers will only lead to a steric stabilization of the particles and chemically interact very little with the particle surface. Experimental evidence for this lack of interaction comes from our work with cobalt nanoparticles.[12] We have demonstrated that cobalt nanoparticles stabilized in PVP and prepared by an organometallic approach display the same magnetization enhancement and magnetic anisotropy, compared to bulk cobalt, as cobalt clusters prepared in high vacuum by time-of-flight experiments. However, the introduction of potential ligands or reactants such as CO, O_2, etc. immediately quenches the magnetism. It is also known from previous work by us and others that the decomposition of $Pt_2(dba)_3$ leads to nanoparticles of various sizes, depending upon the reactive gas (CO or H_2) and the nature of the polymer. An elegant study of CO adsorption on platinum colloids prepared from $Pt_2(dba)_3$ in PVP has recently been reported by de Caro and Bradley.[18] In our case, the particles had been characterized by electron microscopy but not at atomic resolution. We reanalyzed the different systems by HREM and WAXS in order better to understand the systematic errors induced by the different techniques when handling very small particles. We slightly modified the synthetic procedure by carrying out the reactions in a Fischer–Porter bottle under a pressure of 1 bar CO, in the presence of a given polymer, namely polyvinylpyrrolidone (PVP), nitrocellulose (NC) and cellulose acetate (CA). The reaction is rapid under CO and leads to a dark brown solution from which brown precipitates are obtained upon addition to pentane: **Colloid 5** in PVP (3 wt% Pt); **Colloid 6** in NC (2 wt% Pt) and **Colloid 7** in CA (2.5 wt% Pt).

The infrared spectrum of **Colloid 5** was obtained in KBr pellets and consists of two bands at 2043 and 1870 cm⁻¹. No particles were observed by TEM whereas WAXS analysis demonstrates the presence of small crystalline particles having

a fcc structure. The well-defined reduced RDF is consistent with a very small cuboctahedral model and the apparent size of the particles is consistent with a model containing 13 atoms, which generates all the distances observed in the experimental RDF (Fig. 7). The Pt—Pt distance (0.2775 nm) is similar to that found for bulk platinum and a value of 5×10^{-5} nm⁻² has been affected to the individual b_i dispersion factors. Such small particles definitely do not produce sufficient contrast and therefore the negative TEM result should not be considered to be in discrepancy with WAXS.

Colloid 6 shows two bands at 2054 and 1883 cm⁻¹ in the infrared spectrum (KBr pellets). HREM analysis shows well-dispersed particles (Fig. 8) having a mean size of 1.3 nm with a low size dispersity (Fig. 9). Again, a well-defined reduced RDF with a greater coherence length was obtained by WAXS analysis, consistent with a cuboctahedral model (Fig. 10). The structure is fcc and the apparent size of the particles is consistent with a model containing both 55- and 147-atom cuboctahedral particles (in an 85:15 ratio for the best agreement between experimental and simulated data). The Pt—Pt distance had to be adjusted to 0.2760 nm in order to fit the data, which represents a contraction of 0.5% of the Pt—Pt distance. Values of 3×10^{-5} and 8×10^{-5} nm⁻² for the 55- and 147-atom particles were affected to the dispersion factors b_i. This indicates that big particles display a disorder in their outer layer. The diameter of closed-shell clusters of platinum is predicted to be 1.15 nm for a two-shell cluster (55 atoms) and 1.58 nm for a three-shell cluster (147 atoms). Thus, the agreement between both techniques is satisfactory.

Colloid 7 shows two bands at 2049 and 1884 cm⁻¹ in the infrared spectrum (KBr pellets). HREM analysis shows again well-dispersed particles (Fig. 11) having a mean size near 1.7 nm with a very low size dispersity, given the larger size of the particles (Fig. 12). Again, a well-defined reduced RDF was obtained by WAXS analysis, which is consistent with a cuboctahedral model (Fig. 13). The structure is fcc and the apparent size of the particles is consistent with a model containing both 147- and 309-atom cuboctahedral particles in an 80:20 ratio for the best agreement between experimental and simulated data. The Pt—Pt distance had to be adjusted to 0.2745 nm in order to fit the data which represents a contraction of 1% of the Pt—Pt distance. Values of 5×10^{-5} and 15×10^{-5} nm⁻² for the 147- and 309-atom particles were affected to the dispersion factors b_i. This indicates that big particles are disordered in their outer layer. The diameter of closed-shell clusters of platinum is predicted to be 2.02 nm for a four-shell cluster (309 atoms). The agreement between both techniques is satisfactory.

Finally, we prepared a new colloid, **Colloid 8**, by decomposing $Pt_2(dba)_3$ in THF under 3 bar H_2 in the presence of PVP. HREM analysis shows again well-dispersed particles (Fig. 14)
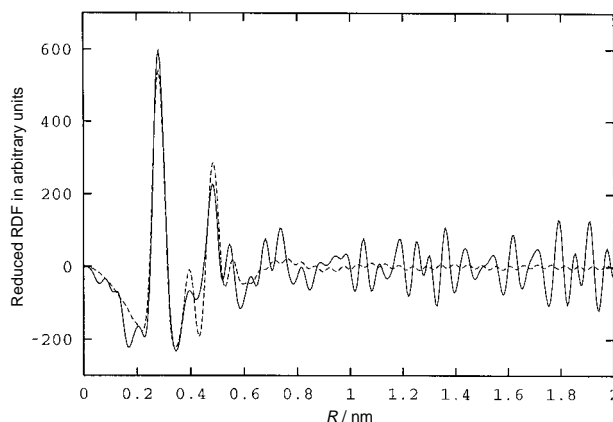

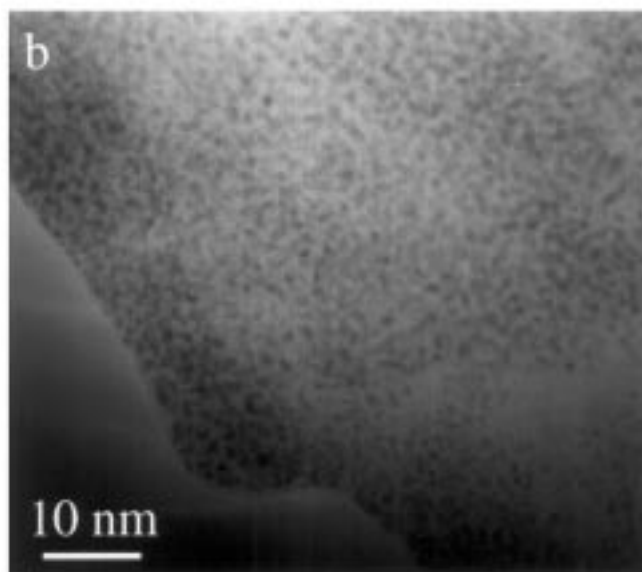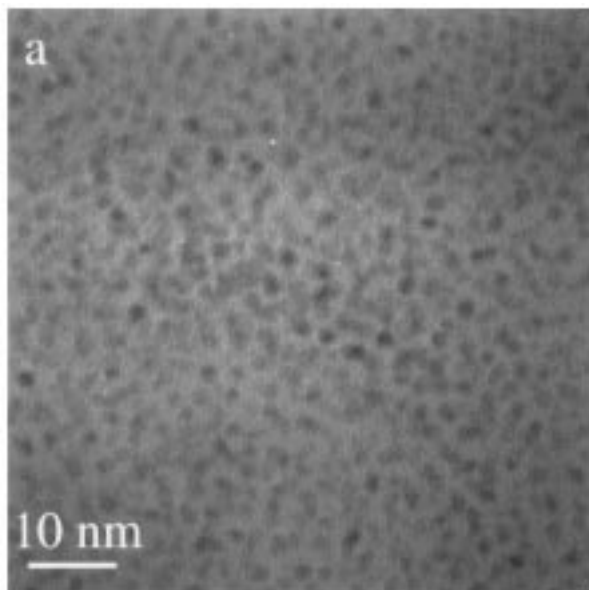**Fig. 7** RDF of particles of **Colloid 5** (solid line, experimental data; broken line, cuboctahedral model at 13 atoms)

Fig. 10 RDF of particles of **Colloid 6** (solid line, experimental data; broken line, function simulated from a mixed-size particle model)

of a mean size near 1.5 nm with a low size dispersity (Fig. 15). A well-defined reduced RDF was obtained by WAXS analysis, which was consistent with a cuboctahedral model as for all other colloids described here (Fig. 16). The structure is fcc and

Fig. 8 (*a*) HREM micrograph of **Colloid 6** showing well-dispersed particles; (*b*) HREM micrograph showing particles imprisoned in a pocket of polymer
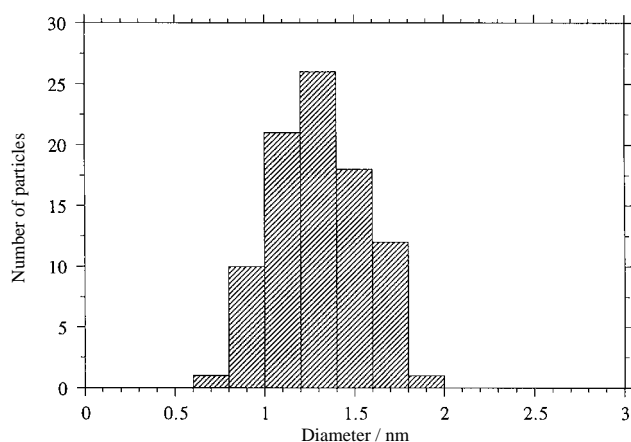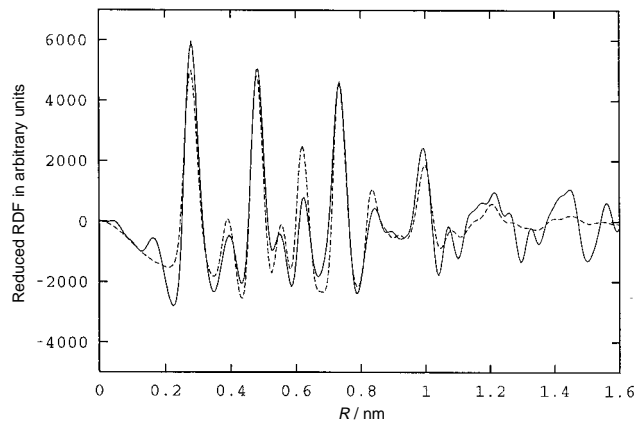

Fig. 9 Histogram of the sizes of **Colloid 6** determined from HREM showing a low size dispersity and a mean size of 1.30 nm
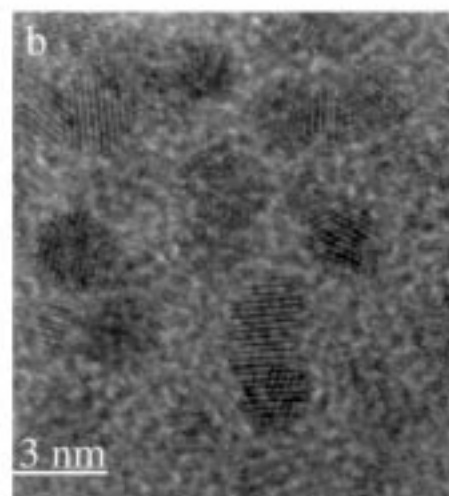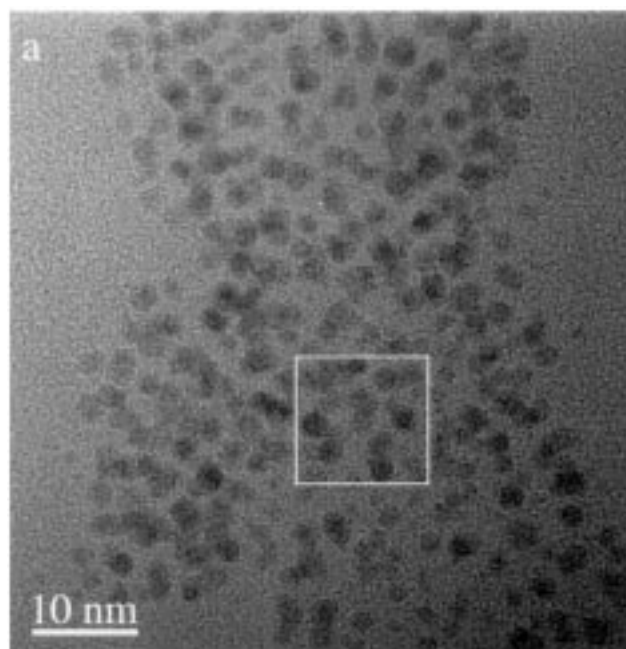

Fig. 11 (*a*) HREM micrograph of **Colloid 7** showing well-dispersed particles; (*b*) HREM image of cuboctahedral platinum particles
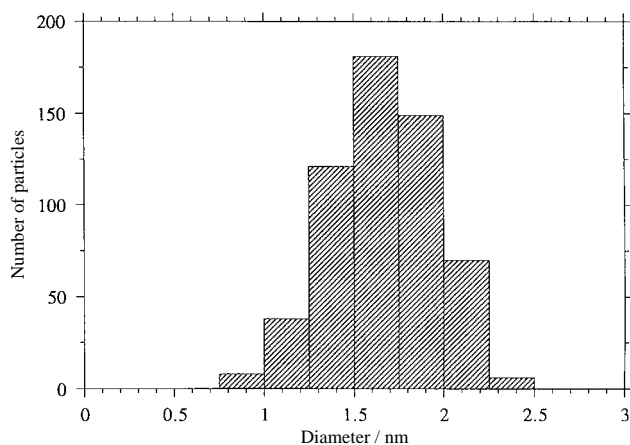
Fig. 12 Histogram of the sizes of **Colloid 7** determined from HREM showing a low size dispersity and a mean size of 1.66 nm

the apparent size of the particles is consistent with a model containing 147 atoms, which generates all the distances observed in the experimental RDF. The Pt—Pt distance had to be adjusted to 0.2740 nm in order to fit the data, which
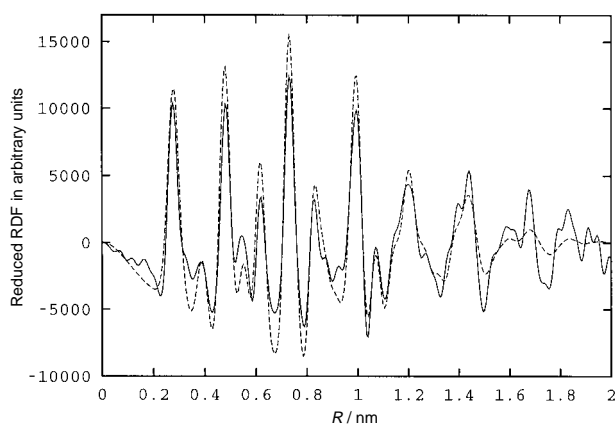

Fig. 13 RDF of particles of **Colloid 7** (solid line, experimental data; broken line, function simulated from a mixed-sized particle model)
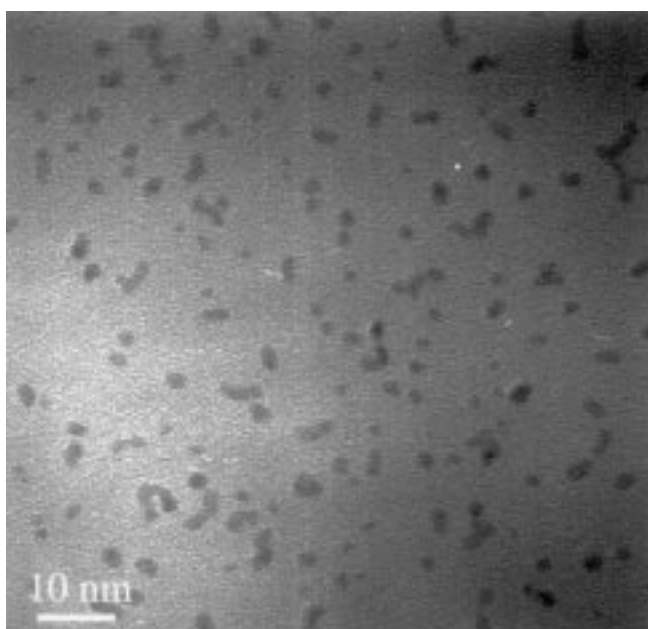

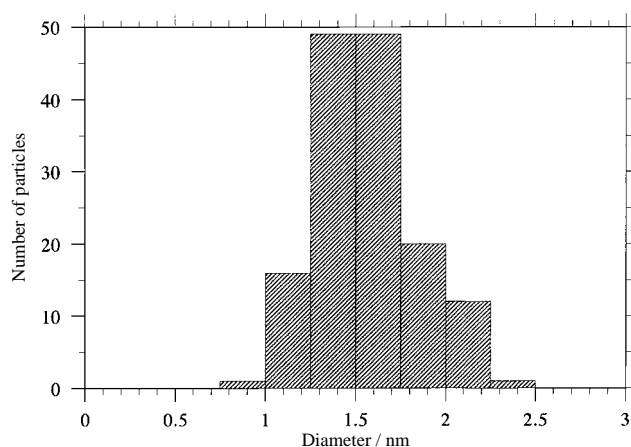Fig. 14 HREM micrograph of **Colloid 8** showing well-dispersed particles

Fig. 15 Histogram of the sizes of **Colloid 8** determined from HREM showing a low size dispersity and a mean size of 1.5 nm
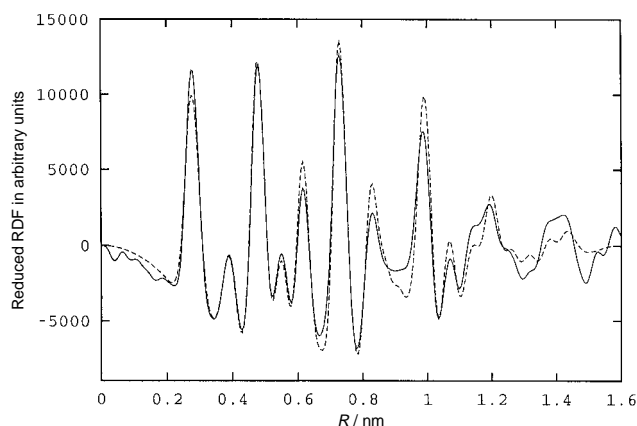

Fig. 16 RDF of particles of **Colloid 8** (solid line, experimental data; broken line, cuboctahedral model at 147 atoms)

represents a contraction of 1.2% of the Pt—Pt distance, and a value of 3×10^{-5} nm^{-2} has been affected to the individual b_i dispersion factors. There is perfect agreement between the HREM and WAXS data.

Discussion

This study provides information on the size variation of the particles as a function of the stabilizer, on the surface of the particles and on the agreement or discrepancy of the WAXS and HREM techniques for the characterization of nanoparticles. These various points will now be discussed.

First, we find good agreement between the WAXS and HREM data in the case of the polymer-stabilized colloids. This agreement is even excellent in the case of **Colloid 8** obtained by decomposition of Pt$_2$(dba)$_3$ in PVP under dihydrogen. We have previously found good agreement between WAXS and HREM data for the characterization of **Colloid 2** stabilized only by THF and CO, but we find a discrepancy between the two techniques when THT is used as a coordinating ligand; this discrepancy becomes even larger when using octanethiol as described in the present study. This observation is not yet fully rationalized but is clearly linked with the presence of coordinating ligands at the surface of the particles. Since what is observed by WAXS is a coherence length, that is the distance at which the positioning of atoms is regular, it is most likely that the outer layer and, in the case of strong ligands such as thiol(ate)s, the next layer are distorted compared to the ideal fcc structure. In the case of colloids that do not contain a strong binding ligand but contain CO, such as **Colloid 6** and **Colloid 7**, it should be noted that the pro-

posed models, which suggest a mixture of two particles sizes, are not exclusive. Even if such models lead to a good fit with the experiment, other models incorporating a greater amount of the larger particles with a more disordered external shell (and therefore not observable by WAXS) should also give close agreement and account for the experimental RDF. For the same reason, fcc models that would not have an overall cuboctahedral structure[19] cannot be rejected, nor demonstrated. The case of the platinum particles obtained in PVP under H$_2$ (**Colloid 8**) is interesting since it gives the best fit between the two techniques. We can also observe by HREM that the particles of this colloid easily coalesce, in agreement with a lack of surface protection. This result is in agreement with those concerning the magnetic properties of cobalt particles prepared from an organometallic precursor under H$_2$ in PVP.[19] In that case the surface of the particle is apparently free and does not interact, at least not significantly, with the polymer and with hydrogen. In contrast, the particles covered by CO are not free particles but start behaving as 'giant clusters'. A similar observation could be made with the Pt—Pt distance: lattice contraction is known to increase when the size of a free particle is reduced.[20] The paradoxal behaviour of a lattice parameter closest to the bulk value for the smallest colloids might be related to a relaxation of the Pt—Pt distance induced by ligand coordination on the surface. The mean Pt—Pt distance would then be related not only to particle size, but also to the presence of ligands on the surface.[21]

The variation of the size of the particles as a function of the polymer, of the ligands and of the decomposition mode is again difficult to rationalize. In the case of decomposition under CO, which is rapid, it is possible that nucleation occurs in pockets of a size specific to each polymer and that the particle growth is limited by the pocket size. When decomposition is slower, such as under H$_2$, the polymer could have time to rearrange to allow the particle to grow further. The change in size induced by the addition of octanethiol to **Colloid 2** could result from an adjustment of the number of thiol(ate) ligands on the surface of the particle.

In summary, this study, and more specifically the comparison between particles of similar size but protected by stabilizers of a different nature, demonstrates the effect of the ligands on the surface of the particles. This surface is the most affected when the coordinating properties of the ligands are the best. By combining different techniques, in this case WAXS and HREM, but also magnetic techniques in other cases, it is possible to gain a realistic view of the particle core and surface structures. It is, however, most important to emphasize that this work describes the synthesis of monodisperse platinum particles containing thiol(ate) ligands, which are stable in solution and in the solid state at room temperature without noticeable decomposition. These particles will now be used as 'super-complexes' for reactivity and 'homogeneous' catalytic studies.

Experimental

General

All operations were carried out using standard Schlenk tube or Fischer–Porter bottle techniques under argon or in a glovebox under nitrogen. Solvents were purified just before use by distillation under a nitrogen atmosphere: THF and toluene over sodium benzophenone, pentane over calcium hydride. All the reactions have been monitored by IR spectroscopy.

Infrared spectra were recorded on a Perkin–Elmer 1725 FT-IR spectrophotometer using KBr pellets when the products were isolated as solids, or as colloidal solutions transferred into a KBr cell. The reference spectrum of the solvent was systematically subtracted.

The octanethiol-stabilized colloidal solutions were prepared by treating a THF or toluene solution of the platinum precursor, Pt$_2$(dba)$_3$, in a Fischer–Porter bottle under 1 bar of CO. The octanethiol ligands were then added. In the case of the polymer-protected platinum particles, the colloidal solutions were obtained by treating a THF solution of the platinum precursor, in a Fischer–Porter bottle under 1 bar of CO or 3 bar of H$_2$, in the presence of the chosen polymer.

NMR spectra were recorded in [^{2}H$_8$]THF on a Bruker AMX 400 operating at 400 MHz for ^{1}H NMR and 100.71 MHz for ^{13}C NMR. The spectra were calibrated using the solvent signals as internal standards, chemical shifts are then given *versus* TMS.

Materials

Pt$_2$(dba)$_3$ was prepared according to literature procedures.[16] Dba, octanethiol, cellulose acetate and PVP were purchased from Aldrich, nitrocellulose from Promochem, K$_2$PtCl$_4$ from Janssen, CO and H$_2$ from Air Liquide; all were used without purification.

TEM experiments. Specimens for TEM studies were prepared by slow evaporation of a drop of suitably diluted colloidal solutions deposited on holey carbon-covered copper grids. The observations were carried out on a Philips CM30/ST electron microscope operated at 300 kV (with a point resolution of 0.19 nm). The size distribution of the particles was determined through numerical analysis of the micrographs. In this procedure, the different particles were first identified according to an upper and lower intensity threshold, then counted and measured. In order to determine the fine structure of the particles, interplanar angles and spacings were measured from numerical diffractograms (Fourier transforms) of HREM images.

WAXS experiments. WAXS measurements were performed on small amounts of the fine powder (obtained after drying) sealed in 1.5 mm diameter Lindemann glass capillaries for **Colloids 5–8**. One measurement was also performed on a concentrated solution of **Colloid 4** in THF, sealed in a 1.0 mm diameter Lindemann glass capillary. Measurements of the X-ray intensity scattered by the samples irradiated with graphite-monochromatized molybdenum K$_\alpha$ (0.071 069 nm) radiation were performed using a dedicated two-axis diffractometer. The air-scattering background was small enough to be neglected. Time for data collection was typically 20 h for a set of 457 measurements at room temperature in the range $0° < \theta < 65°$ for equidistant s values [$s = 4\pi(\sin\theta/\lambda)$]. Fluorescence from the platinum was corrected by using a profile obtained from two measurements collected from the same sample with and without aluminium filters. In order to separate the intensity related to the particles from contributions generated by other components (polymer, solvent, empty capillary), scattering patterns from an empty capillary and one filled with solvent or polymer alone were also collected under the same conditions. The raw intensity was then corrected for the capillary and polymer or THF contributions, attenuated by sample absorption. Polarization and self-absorption corrections were also applied. Data were reduced[22] in order to extract the structure-related component of WAXS, the so-called reduced intensity function $i(s)$, and Fourier-transformed to allow for RDF analysis, using the formula

$$F(r) = \frac{2r}{\pi} \int_{s_{min}}^{s_{max}} s \cdot i(s)\sin(r \cdot s)\mathrm{d}s$$

where $F(r)$ is actually a reduced RDF whose maximum for a given r value indicates that at least two atoms in an elementary volume are separated by the distance r. Analysis of the experimental function clearly pointed out the fcc structure and

provided an approximate measurement of the metal–metal bond length and of the order extent inside the particles. To investigate the structure further, a model was then defined in order to compute theoretical functions for the intensity and radial distribution *via* Debye's formula

$$i_D(s) = 2 \sum_{i=1}^{N-1} \sum_{j=i+1}^{N} f_i(s) \cdot f_j(s)$$

$$\times \frac{\sin(s \cdot r_{ij})}{s \cdot r_{ij}} \exp(-b_{ij} \cdot s^2)$$

where N is the total number of atoms in the model, f_i the atomic scattering factor for atom i, r_{ij} the distance between atoms i and j and b_{ij} a dispersion factor affecting the $i - j$ interaction).

Best values of the parameters defining the models were estimated from the agreement reached between experimental and computed RDF but also between the related reduced intensity functions. All models were built cuboctahedral in shape and the b_{ij} factors were set to a same value for all atoms in the particle since individual adjustment of atomic positions and dispersions requires additional information. This somewhat crude model, where no difference is made between core and surface atoms, is convenient for comparing one system to another. No more than two different sizes of particles were included to fit the experiments.

Compounds

Colloids 1 and 3. Colloid 1 was prepared as described in a preceding paper[10] and the octanethiol ligand was added subsequently to obtain **Colloid 3** as described below.

A solution of Pt$_2$(dba)$_3$ (130 mg, 0.12 mmol) in 40 mL of freshly distilled and degassed toluene in a Fischer–Porter bottle was pressurized with 1 bar of CO during 20 min under vigorous stirring. During this time the solution changed color from deep purple to brown and a reddish-brown solid precipitated. The solution was removed by filtration and the precipitate was washed with toluene (30 mL) and pentane (6 × 30 mL) until the solution turned colorless (to eliminate dba) and dried under vacuum. **Colloid 1** IR (KBr, cm^{-1}): 2052, 1811.

A toluene solution of octanethiol (6 μL, 0.035 mmol, 5 mL toluene, 0.2 equiv. per Pt) was then added to **Colloid 1**. The mixture was subjected to ultrasound in a bath for 1 h and left stirring in solution for 3 days, leading to **Colloid 3**. Infrared spectra were recorded during this period of time. **Colloid 3**: IR (toluene, cm^{-1}): 2051 and 1811 after 2 h; 2047 after 2 days and 2039 after 3 days. After evaporation to dryness, **Colloid 3** was isolated as a sticky brown product and could not be analyzed by microanalysis. HREM analysis: size distribution: 0.75–2.75 nm, mean size: 1.4 nm.

Colloids 2 and 4. Colloid 2 was also obtained as mentioned in a precedent publication[10] and a solution of the octanethiol ligand was added subsequently to form **Colloid 4**.

A solution of Pt$_2$(dba)$_3$ (310 mg, 0.28 mmol) in 75 mL THF was prepared and transferred into a Fischer–Porter bottle by a Teflon canula. The bottle was then carefully evacuated and pressurized with 1 bar of CO during 20 min under vigorous stirring. The color of the mixture changed rapidly from violet to brown and the medium remained homogeneous. Then the mixture was transferred, filtered and evaporated to dryness. The brown residue was washed with pentane to eliminate dba (6 × 30 mL; until the pentane solution turned colorless) and dried under vacuum. **Colloid 2** IR (THF, cm^{-1}): 2052, 1810.

A THF solution of octanethiol (15 μL, 0.086 mmol, 5 mL THF, 0.2 equiv. per Pt) was then added to **Colloid 2**. The dissolution of this platinum precursor was very fast and the resulting mixture was a homogeneous brown solution. **Colloid 4** IR (THF, cm^{-1}): 2040 and 1799. After evaporation to

dryness, **Colloid 4** was isolated as a brown powder. Microanalysis: C, 44.00, H, 4.38, S, 1.29, Pt, 34.05%, S : Pt, 4.34 : 1. HREM analysis: fcc particles, size distribution: 1.0–2.25 nm, mean size: 1.6 nm.

Colloid 5*: Pt/PVP/CO.* To a solution of Pt$_2$(dba)$_3$ (65 mg, 0.056 mmol) in 20 mL of freshly distilled and degassed THF in a Fischer–Porter bottle, a solution of PVP (436 mg; 20 mL of THF) was added. The mixture was then submitted to a pressure of 1 bar of CO during 10 min under vigorous stirring. During this time the solution color changed from violet to brown and the colloid precipitated. The reaction mixture was washed with pentane (6 × 30 mL, until the solution turned colorless) to eliminate dba. It was then filtered and the solid residue was dried under vacuum. IR (KBr, cm^{-1}): 2043, 1870. Microanalysis: Pt : PVP = 3 wt%. HREM analysis: no particles were observed.

Colloid 6: Pt/NC/CO. To a solution of Pt$_2$(dba)$_3$ (44 mg, 0.040 mmol) in 20 mL of freshly distilled and degassed THF in a Fischer–Porter bottle, a THF solution of NC (307 mg; 20 mL of THF) was added. The mixture was then submitted to a pressure of 1 bar of CO during 10 min under vigorous stirring. During this time, the solution color changed rapidly from violet to dark brown and stayed homogeneous. The reaction mixture was washed with pentane (6 × 30 mL, until the solution turned colorless) to favour the precipitation of the colloid and eliminate dba. It was then filtered and the brown solid was evaporated to dryness. IR (KBr, cm^{-1}): 2054, 1883. Microanalysis: Pt : NC = 2 wt%. HREM analysis: fcc particles, size: 0.6–2.0 nm, mean size: 1.3 nm.

Colloid 7: Pt/CA/CO. To a solution of Pt$_2$(dba)$_3$ (45 mg, 0.041 mmol) in 20 mL of freshly distilled and degassed THF in a Fischer–Porter bottle, a THF solution of CA (322 mg; 20 mL of THF) was added. The mixture was then submitted to a pressure of 1 bar of CO during 10 min under vigorous stirring. During this time, the color of the mixture changed rapidly from violet to dark brown and stayed homogeneous. The reaction mixture was washed with pentane (6 × 30 mL, until the solution turned colorless) to favour the precipitation of the colloid and eliminate dba. It was then filtered and the brown residue was evaporated to dryness. IR (KBr, cm^{-1}): 2049, 1884. Microanalysis: Pt : CA = 2.5 wt%. HREM analysis: fcc particles, size: 0.75–2.5 nm, mean size: 1.7 nm.

Colloid 8: Pt/PVP/H$_2$. To a solution of Pt$_2$(dba)$_3$ (164 mg, 0.150 mmol) in 35 mL of freshly distilled and degassed THF in a Fischer–Porter bottle, a solution of PVP (881.5 mg; 60 mL of THF) was added. The mixture was then submitted to a pressure of 3 bar of H$_2$ during 3 days under vigorous stirring. During this time the color of the reaction mixture changed from violet to black and the colloid precipitated. The solution was removed by filtration. The solid residue was dissolved with methyl alcohol (15 mL) and then precipitated by addition of 50 mL of pentane, filtered and washed with 15 mL of pentane before drying under vacuum. IR (KBr, cm^{-1}): 2043, 1870. Microanalysis: Pt : PVP = 12.51 wt%. HREM analysis: fcc particles, size: 0.75–2.5 nm, mean size: 1.5 nm.

References

1 *Clusters and Colloids, from Theory to Applications*, ed. G. Schmid, VCH, Weinheim, 1994.
2 L. N. Lewis, *Chem. Rev.*, 1993, **93**, 2693.
3 J. S. Bradley, in ref. 1, ch. 6, pp. 459–544.

4 *Nanotechnology, Molecularly Designed Materials*, ed. G.-M. Chow and K. E. Gonsalves, ACS Symposium Series 622, American Chemical Society, Washington DC, 1996.

5 (*a*) T. Vossmeyer, E. DeIonno and J. R. Heath, *Angew. Chem., Int. Ed. Engl.*, 1997, **36**, 1080; (*b*) T. Sato, D. Brown and B. F. G. Johnson, *Chem. Commun.*, 1997, 1007; (*c*) M. J. Hostetler, and R. W. Murray, *Curr. Opin. Colloid Interface Sci.*, 1997, **2**, 42; (*d*) C. S. Weisbecker, M. V. Merritt and G. M. Whitesides, *Langmuir*, 1996, **12**, 3763; (*e*) M. Brust, D. Bethell, D. J. Schiffrin and C. J. Kiely, *Adv. Mater.*, 1995, **7**, 795.

6 (*a*) M. T. Reetz, M. Winter and B. Tesche, *Chem. Commun.*, 1997, 147; (*b*) P. C. Ohara, J. H. Heath and W. M. Gelbart, *Angew. Chem., Int. Ed. Engl.*, 1997 **36**, 1078; (*c*) A. Taleb, C. Petit and M. P. Pileni, *Chem. Mater.*, 1997, **9**, 950; (*d*) L. Wenjie, J. A. Virtanen and R. M. Penner, *Langmuir*, 1995, **11**, 4361.

7 (*a*) X. Peng, T. E. Wilson, A. P. Alivisatos and P. G. Schultz, *Angew. Chem., Int. Ed. Engl.*, 1997, **36**, 145; (*b*) X. Peng, M. C. Schlamp, A. V. Kadavanich and A. P. Alivisatos, *J. Am. Chem. Soc.*, 1997, **119**, 7019.

8 (*a*) J. S. Bradley, J. M. Millar, E. W. Hill, C. Klein, B. Chaudret and A. Duteil, *Faraday Discuss. Chem. Soc.*, 1991, **92**, 255; (*b*) D. de Caro, H. Wally, C. Amiens and B. Chaudret, *J. Chem. Soc., Chem. Commun.*, 1994, 1891; (*c*) C. Amiens, D. de Caro, B. Chaudret, J. S. Bradley, R. Mazel and C. Roucau, *J. Am. Chem. Soc.* 1993, **115**, 11638; (*d*) D. de Caro, V. Agelou, A. Duteil, B. Chaudret, R. Mazel, C. Roucau and J. S. Bradley, *New J. Chem.*, 1995, **19**, 1265; (*e*) D. de Caro, T. Ould Ely, A. Mari, B. Chaudret, E. Snoeck, M. Respaud, J.-M. Broto and A. Fert, *Chem. Mater.*, 1996, **8**, 1987.

9 A. Duteil, R. Quéau, B. Chaudret, R. Mazel, C. Roucau and J. S. Bradley, *Chem. Mater.*, 1993, **5**, 341.

10 A. Rodriguez, C. Amiens, B. Chaudret, M.-J. Casanove, P. Lecante and J. S. Bradley, *Chem. Mater.*, 1996, **8**, 1978.

11 M. Bardaji, O. Vidoni, A. Rodriguez, C. Amiens, B. Chaudret, M.-J. Casanove and P. Lecante, *New J. Chem.*, 1997, **21**, 1243.

12 J. Osuna, D. de Caro, C. Amiens, B. Chaudret, E. Snoeck, M. Respaud, J.-M. Broto and A. Fert, *J. Phys. Chem.*, 1996, **100**, 14571.

13 (*a*) R. S. Ingram, M. J. Hostetler and R. W. Murray, *J. Am. Chem. Soc.*, 1997, **119**, 9175; (*b*) S. J. Green, J.-J. Stokes, M. J. Hostetler, J. J. Pietron and R. W. Murray, *J. Phys. Chem.*, 1997, **101**, 2663; (*c*) P. A. Buining, B. M. Humbel, A. P. Philipse and A. J. Verkleij, *Langmuir*, 1997, **13**, 3921; (*d*) A. Badia, L. Cuccia, L. Demers, F. Morin and R. B. Lannox, *J. Am. Chem. Soc.*, 1997, **119**, 2682; (*e*) S. R. Johnson, S. D. Evans, S. W. Mahon and A. Ullman, *Langmuir*, 1997, **13**, 51; (*f*) A. Badia, S. Singh, L. Demers, L. Cuccia, G. R. Brown and R. B. Lannox, *Chem. Eur. J.*, 1996, **2**, 359; (*g*) M. Hostetler, S. J. Green, J. J. Stokes and R. W. Murray, *J. Am. Chem. Soc.*, 1996, **118**, 4212; (*h*) M. Hostetler, J. J. Stokes and R. W. Murray, *Langmuir*, 1996, **12**, 3604; (*i*) R. L. Whetten, J. T. Khoury, M. M. Alvarez, S. Murthy, I. Vezmar, Z. L. Wang, P. W. Stephens, C. L. Cleveland, W. D. Luedte and U. Landman, *Adv. Mater.*, 1996, **8**, 428; (*j*) R. H. Terrill, T. A. Postlethwaite, C.-H. Chen, C.-D. Poon, A. Terzis, A. Chen, J. E. Hutchinson, M. R. Clark, G. Wignall, J. D. Londono, R. Superfine, M. Falvo, C. S. Johnson Jr., E. T. Samulski and R. W. Murray, *J. Am. Chem. Soc.*, 1995, **117**, 12537; (*k*) M. Brust, J. Fink, D. Bethell, D. J. Schiffrin and C. Kiely, *J. Chem. Soc., Chem. Commun.*, 1995, 1655; (*l*) M. Brust, M. Walker, D. Bethell, D. J. Schiffrin and R. Whyman, *J. Chem. Soc., Chem. Commun.*, 1994, 801; (*m*) M. D. Porter, T. B. Bright, D. L. Allara and C. E. D. Chidsey, *J. Am. Chem. Soc.*, 1987, **119**, 2682.

14 A. Badia, W. Gao, S. Singh, L. Demers, L. Cuccia and L. Reven, *Langmuir*, 1996, **12**, 1262.

15 K. V. Sarathy, G. U. Kulkarni and C. N. R. Rao, *Chem. Commun.*, 1997, 537.

16 K. Moseley and P. M. Maitlis, *J. Chem. Soc., Chem. Commun.*, 1971, 982.

17 The estimation of particle size distributions required the measurement of a large number of particles (*ca.* 400, see Fig. 2, 5, 9, 12, 15). The whole procedure of measuring the particles was made according to a classical method. The particles were measured on micrographs that were taken 'in focus', where the carbon film displays a much more uniform gray contrast than in the high resolution (defocussed) micrographs. A statistical distribution was obtained using quantitative analysis software (OPTIMAS). The standard error was estimated to be ± 0.15 nm.

18 D. de Caro and J. S. Bradley, *Langmuir*, in press.

19 J. D. Roth, G. J. Lewis, L. K. Safford, X. Jiang, L. F. Dahl and M. J. Weaver, *J. Am. Chem. Soc.*, 1992, **114**, 6159.

20 S. N. Khanna, J. P. Bucher, J. Buttet and F. Cyrot-Lackmann, *Surf. Sci.*, 1983, **127**, 165.

21 B. Moraweck and A. J. Renouprez, *Surf. Sci.*, 1981, **106**, 35.

22 M.-J. Casanove, P. Lecante, E. Snoeck, A. Mosset and C. Roucau, *J. Phys. III (France)*, 1997, **7**, 505,